

Modeling still matters: a surprising instance of catastrophic floating point errors in mathematical biology and numerical methods for ODEs

Cordula Reisch^{*1} and Hendrik Ranocha^{†2}

¹Institute for Partial Differential Equations, TU Braunschweig, Germany

²Applied Mathematics, University of Hamburg, Germany Present address: Institute of Mathematics, Johannes Gutenberg University Mainz, Germany.

October 05, 2024

We guide the reader on a journey through mathematical modeling and numerical analysis, emphasizing the crucial interplay of both disciplines. Targeting undergraduate students with basic knowledge in dynamical systems and numerical methods for ordinary differential equations, we explore a model from mathematical biology where numerical methods fail badly due to catastrophic floating point errors. We analyze the reasons for this behavior by studying the steady states of the model and use the theory of invariants to develop an alternative model that is suited for numerical simulations. Our story intends to motivate combining analytical and numerical knowledge, even in cases where the world looks fine at first sight. We have set up an online repository containing an interactive notebook with all numerical experiments to make this study fully reproducible and useful for classroom teaching.

Key words. mathematical modeling, steady states, dynamical systems, numerical instability, invariants, Runge-Kutta methods

AMS subject classification. 37M05, 65L06, 65L20, 65P40, 97D40

1 Introduction

Setting up a nice mathematical model for some applications, using a proper numerical scheme for solving the differential equations — and wondering what is happening? Oftentimes, mathematical models of ordinary differential equations (ODEs) are easily solvable numerically as long as a suitable scheme is used. In this report, we tell a different story, which highlights the process of setting up a model and analyzing it properly for ensuring trustable and correct numerical solutions.

This article intends to take the reader on a small journey through the interplay between modeling, numerical simulation and analysis. We will pass a biological motivation on the inheritance of genes like the inheritance of flower colors, and set up a mathematical model of ODEs that describes the proportions of different genotypes in the total population. As a next step, we try to get a first

^{*}ORCID: 0000-0003-1442-1474

[†]ORCID: 0000-0002-3456-2277

impression of the system's behavior by running numerical simulations that are expected to show the time-dependent dynamics of the system. The first plot twist is on the goodwill and trust concerning numerical simulation, even when the schemes are chosen wisely. We discover the reasons for the strange simulations by changing the focus of research from numerical analysis to dynamical system analysis and analyzing the steady states of the dynamical system. The curtains fall for the theory of invariants. The friendly-looking model for inheritance turns out to conserve an important quantity — the total population — as a second integral. Accumulating floating point errors reveal the instability of steady states. By changing the system, we turn the total population into a first integral. The new model reacts in a stable way to floating point errors and trust in numerical simulations is restored.

Please use our story to motivate combining analytical and numerical knowledge, even in cases where no problems are expected. A related story focusing on step size control of numerical ODE solvers is published by Skufca [24], which we used as an inspiration for the title of this report. To make this study fully reproducible, we have set up an online repository [20] containing an interactive notebook with all numerical experiments using the modern programming language Julia.

Before starting our journey, we would like to highlight the aim of this article. The intention is not to provide new mathematical results but to motivate students from a modeling perspective why a deeper dive into mathematical analysis is helpful and provides much insight. Therefore, we refer to analytical results rather from a modeling perspective emphasizing the nature of the problems, and we include references for further studies in the end. The outlook will include literature on the theory of ordinary differential equations on manifolds with local coordinates and numerical correction schemes, further modeling examples, and structure-preserving numerical methods. During the story, the focus will be on the applied modeling perspective.

2 Modeling the inheritance of genes

Mathematical biologists strive for explaining life in mathematical terms by abstracting from individuals and finding general insight into complex processes. One big question of life is the inheritance of genes and therefore the evolution of populations. Here, we model how genes are passed on from a parent generation to the next generation. While reading, you can have in mind flowers with different possible colors like white, rose and red, or any example where two copies of a gene are present. Such an organism is called diploid. Different versions of a gene are called alleles. We consider here two different alleles, either X or x . Possible combinations give the genotypes XX , Xx and xx . If every parent inherits one of its alleles, the genotypes of the next generation are given according to the probabilities of the alleles in the parent generation. The formulation of generations implies a discrete time, see for example [4, Chapter 4]. In this setting, we assume all processes to be time continuous with blurred generations. The assumption of blurred generations in continuous time is in particular relevant for longer timescales. On short timescales, these assumptions are too strong and lead to an unfeasible model. Here, we are interested in describing the genetic drift, which is the change of the allele and gene distribution in a population.

In this model, the population is divided into compartments c_i according to their genotypes. Let c_1 be the compartment of the genotype XX , c_2 the compartment for the mixed genotype Xx , and c_3 the compartment of xx . The size of each compartment is time-depending.

The inheritance of the genotypes is given by Mendel's Law of Segregation in Table 1. The genotypes of the outcomes depend on the genotypes of the parents' generation: Every offspring inherits one allele of each parent, e.g., an offspring has the genotype c_1 if parents with XX alleles or Xx alleles mix. The probabilities of passing on the genotypes are given in Table 1.

Table 1 can be read in the example of flower colors as follows: If XX is the red flower genotype, c_1 gives the number of red flowers; Xx is the rose genotype with compartment c_2 and xx is the white genotype with compartment c_3 . If the parents are of genotype XX and Xx , the offspring is red with probability $1/2$ (genotype c_1 , XX), and rose with probability $1/2$ (genotype c_2 , Xx).

Table 1: Mendel's Law of Segregation: Probability of the genotypes of the offsprings depending on the parents genotypes XX , Xx , xx with their compartments c_1, c_2, c_3 .

	$c_1 [XX]$	$c_2 [Xx]$	$c_3 [xx]$
$c_1 [XX]$	$c_1: 1$	$c_1: 1/2, c_2: 1/2$	$c_2:1$
$c_2 [Xx]$	$c_1:1/2, c_2:1/2$	$c_1: 1/4, c_2: 1/2, c_3:1/4$	$c_2: 1/2, c_3:1/2$
$c_3 [xx]$	$c_2:1$	$c_2: 1/2, c_3: 1/2$	$c_3: 1$

Following these mixing rules, Mendel's Law of Segregation can be transformed into ordinary differential equations, compare [11], for the genotype compartments c_i , namely

$$\begin{aligned} c_1' &= \frac{g(c_{\text{sum}})}{c_{\text{sum}}^2} \left(c_1^2 + c_1 c_2 + \frac{1}{4} c_2^2 \right), \\ c_2' &= \frac{g(c_{\text{sum}})}{c_{\text{sum}}^2} \left(\frac{1}{2} c_2^2 + c_1 c_2 + 2c_1 c_3 + c_2 c_3 \right), \\ c_3' &= \frac{g(c_{\text{sum}})}{c_{\text{sum}}^2} \left(\frac{1}{4} c_2^2 + c_2 c_3 + c_3^2 \right), \end{aligned} \quad (2.1)$$

where $g(c_{\text{sum}}) \geq 0$ is a growth function for the whole population $c_{\text{sum}} = c_1 + c_2 + c_3$.

In model (2.1), all genotypes have the same growth rate. The factor $1/c_{\text{sum}}^2$ normalizes the equations such that the overall growth is a function of the total population c_{sum} ,

$$c_1' + c_2' + c_3' = \frac{g(c_{\text{sum}})}{c_{\text{sum}}^2} \left(c_1^2 + c_2^2 + c_3^2 + 2c_1 c_2 + 2c_1 c_3 + 2c_2 c_3 \right) = \frac{g(c_{\text{sum}})}{c_{\text{sum}}^2} (c_1 + c_2 + c_3)^2, \quad (2.2)$$

resulting in $c_{\text{sum}}' = g(c_{\text{sum}})$. Other dynamics of the compartments like mutation, mortality, or fitness are not regarded here, but for example in Langemann, Richter and Vollrath [11], Britton [4], and Allen and McAvoy[1]. Those variations of models include for example the assumption of genotype-specific growth rates depending on the fitness which effects the assumptions in (2.1).

The equations in system (2.1) can be written as well in a matrix vector formalism [11] using $c = (c_1, c_2, c_3)^T$ and the inheritance matrices

$$W_1 = \begin{pmatrix} 1 & \frac{1}{2} & 0 \\ \frac{1}{2} & \frac{1}{4} & 0 \\ 0 & 0 & 0 \end{pmatrix}, \quad W_2 = \begin{pmatrix} 0 & \frac{1}{2} & 1 \\ \frac{1}{2} & \frac{1}{2} & \frac{1}{2} \\ 1 & \frac{1}{2} & 0 \end{pmatrix}, \quad W_3 = \begin{pmatrix} 0 & 0 & 0 \\ 0 & \frac{1}{4} & \frac{1}{2} \\ 0 & \frac{1}{2} & 1 \end{pmatrix} \quad (2.3)$$

with $W_1 + W_2 + W_3 = \mathbb{1}_{3 \times 3}$ (the matrix in $\mathbb{R}^{3 \times 3}$ with all entries equal to unity). Then

$$c_i' = \frac{g(c_{\text{sum}})}{c_{\text{sum}}^2} c^T W_i c \quad (2.4)$$

gives system (2.1).

Due to the growth function $g(c_{\text{sum}}) > 0$, the total population grows. Regarding long-term phenomena, this assumption of unlimited growth is unrealistic. Therefore, and to focus on the drift effect of the mutations, we change the modeling objective to a situation with conserved quantities. From a biological point of view, both the absolute number of copies and proportions of genotypes are of interest. The genotype proportions $q_i = c_i/c_{\text{sum}}$ at a certain time t can be estimated by collecting and evaluating samples. Using the product rule and (2.4), the dynamics of the proportions q_i are given indirectly by

$$c_i' = q_i' c_{\text{sum}} + q_i c_{\text{sum}}'. \quad (2.5)$$

The change of the total population is given by the growth function, $c'_{\text{sum}} = g(c_{\text{sum}})$ and the change of c_i is given by (2.4). Therefore, the genotype proportions $q = (q_1, q_2, q_3)^T$ follow

$$q'_i = \frac{g(c_{\text{sum}})}{c_{\text{sum}}^3} \left(c^T W_i c \right) - q_i \frac{g(c_{\text{sum}})}{c_{\text{sum}}} = \frac{g(c_{\text{sum}})}{c_{\text{sum}}} \left(q^T W_i q - q_i \right). \quad (2.6)$$

For the special choice of exponential growth $g(c_{\text{sum}}) = c_{\text{sum}}$, this becomes

$$q'_i = f_i(q) = q^T W_i q - q_i, \quad i \in \{1, 2, 3\}, \quad (2.7)$$

or written as a system

$$\begin{aligned} q'_1 &= q_1^2 + q_1 q_2 + \frac{1}{4} q_2^2 - q_1, \\ q'_2 &= \frac{1}{2} q_2^2 + q_1 q_2 + 2 q_1 q_3 + q_2 q_3 - q_2, \\ q'_3 &= \frac{1}{4} q_2^2 + q_2 q_3 + q_3^2 - q_3. \end{aligned} \quad (2.8)$$

The initial conditions $q_1(0) = q_{01}$, $q_2(0) = q_{02}$ and $q_3(0) = q_{03}$ should fulfill $q_i(0) \in [0, 1]$ and

$$q_{\text{sum}}(0) = \sum_{i=1}^3 q_i(0) = 1$$

since q_i describe the proportions of the different genotypes in the whole population. We investigate the time-dependent dynamics of the genotypes in the population.

There are basically two paths one can follow from here on. The “ideal” way begins with a mathematical analysis of the model; if everything is well-understood qualitatively and the model behaves as expected, numerical simulations can be used with confidence to gain a quantitative understanding of the dynamics. Here, we follow the “practical” approach chosen probably in most cases by practitioners: We directly perform numerical simulations to get a basic understanding of the model; based on the numerical results, we will focus our attention on interesting behavior for a deeper mathematical analysis.

2.1 Numerical experiments

All numerical experiments presented in this article are available from our reproducibility repository [20]. In particular, an interactive Pluto.jl [16] notebook based on Julia [2] is available for download.

Numerical simulations provide a first impression of the spread of the genotypes over time. At first, we use the fifth-order Runge-Kutta method of Tsitouras [27], which is the recommended default method for non-stiff problems in OrdinaryDiffEq.jl [17]. As shown in Figure 1, the numerical solution appears to converge to a steady state — until it suddenly goes to zero. While the tendency towards the steady state matches our expectation, the decay to zero contradicts the modeling assumption $\sum_i q_i = 1$ and does not change significantly if we use stricter tolerances — the time of “extinction” may only be postponed a bit.

The method of Tsitouras is tested quite well in practice. But maybe something is wrong with it for this specific problem? To double-check the results, we also apply the classical fifth-order method of Dormand and Prince [5] well-known from ode45 in MATLAB [23]. The short-term results shown in Figure 2 are the same as before. However, this time the numerical solutions blow up instead.

The results for both methods do not change significantly if we use stricter tolerances. We have also tested other methods (explicit and implicit Runge-Kutta methods, Rosenbrock-type methods, multistep methods) implemented in a variety of software packages and programming languages. The results are all similar to the two prototypical examples shown above — both contradicting the behavior we expected from the models. This is certainly something we need to understand, in particular for studying the fixation or loss of alleles or genotypes over a longer timeframe.

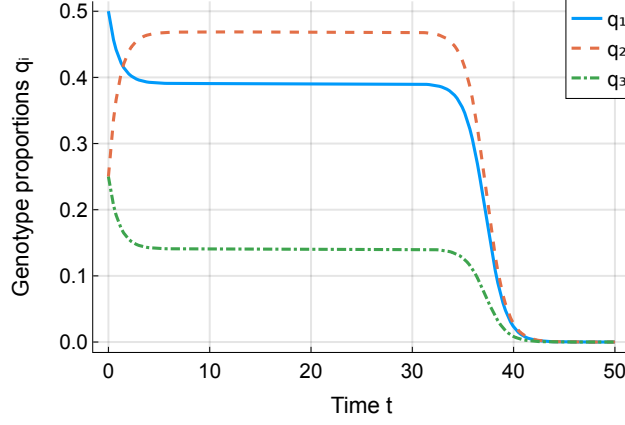


Figure 1: Numerical solution of the system (2.8) with initial condition $q_0 = (0.5, 0.25, 0.25)^T$ obtained by the fifth-order Runge-Kutta method of Tsitouras [27] implemented in OrdinaryDiffEq.jl [17] in Julia [2] with absolute and relative tolerances 10^{-8} .

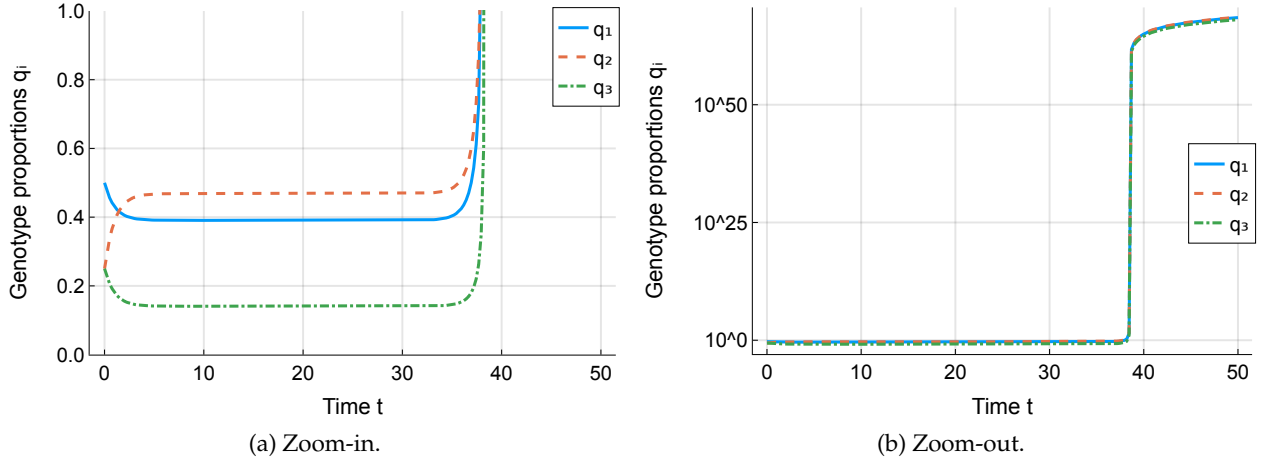


Figure 2: Numerical solution of the system (2.8) with initial condition $q_0 = (0.5, 0.25, 0.25)^T$ obtained by the fifth-order Runge-Kutta method of Dormand and Prince [5] implemented in OrdinaryDiffEq.jl [17] in Julia [2] with absolute and relative tolerances 10^{-8} . (a) Focus on the tendency towards steady states, (b) Change of the system behavior to blow up.

3 Dynamical system analysis

As numerical simulations show surprising behavior of the solutions, we have a deeper look at the analysis of the dynamical systems. The aim is to understand why the numerical simulations fail and to get ideas on how to overcome these difficulties by changing the system.

3.1 A reduced 2-component model

For some easier visualization, we regard an inheritance model for only two genotypes (q_1 and q_2) and one allele, including some mutation. In the example of studying flower colors, the two genotypes could be yellow and orange flowers that do not mix their color. The mutation describes an outcome of genotype q_i if the parent generation has the genotype q_j with $i \neq j$. Given a parameter $a \in (0, 1)$, the dynamics read

$$\begin{aligned} q_1' &= f_1(q) = a q_1^2 + q_1 q_2 + (1 - a) q_2^2 - q_1, \\ q_2' &= f_2(q) = (1 - a) q_1^2 + q_1 q_2 + a q_2^2 - q_2. \end{aligned} \quad (3.1)$$

The vector field visualization in Figure 3 illustrates the dynamics of the system.

The system (3.1) has two steady states, $(0, 0)^T$ and $(1/2, 1/2)^T$, where only the latter fulfills the conservation condition $q_{\text{sum}} = q_1 + q_2 = 1$ and therefore lies on the hyperplane given by $q_2 = 1 - q_1$. This line represents an invariant manifold for q_{sum} fulfilling the conservation condition. The trivial steady state $q^* = 0$ is stable while the non-trivial steady state is unstable. Figure 3 shows this behavior since initial values with $q_1 + q_2 < 1$ have trajectories leading to the trivial steady state. Initial conditions with $q_1 + q_2 > 1$ have trajectories with $\lim_{t \rightarrow \infty} q_i(t) = \infty$.

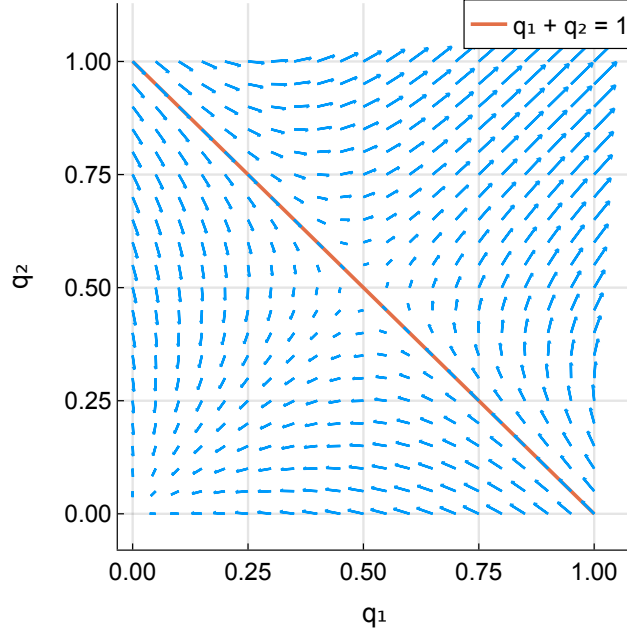


Figure 3: Visualization of the vector field f of the 2-component system (3.1) with $a = 0.7$. The invariant manifold given by $q_1 + q_2 = 1$ is highlighted. The length of the lines is proportional to $\sqrt{\|f(q)\|}$.

Numerical solutions of (3.1) behave qualitatively similar to their analogs for the 3-component model (2.8): The numerical solutions shown in Figure 4 seem to converge to the (unstable) steady state $(1/2, 1/2)^T$ at first but eventually go to zero (the stable steady state) or blow up.

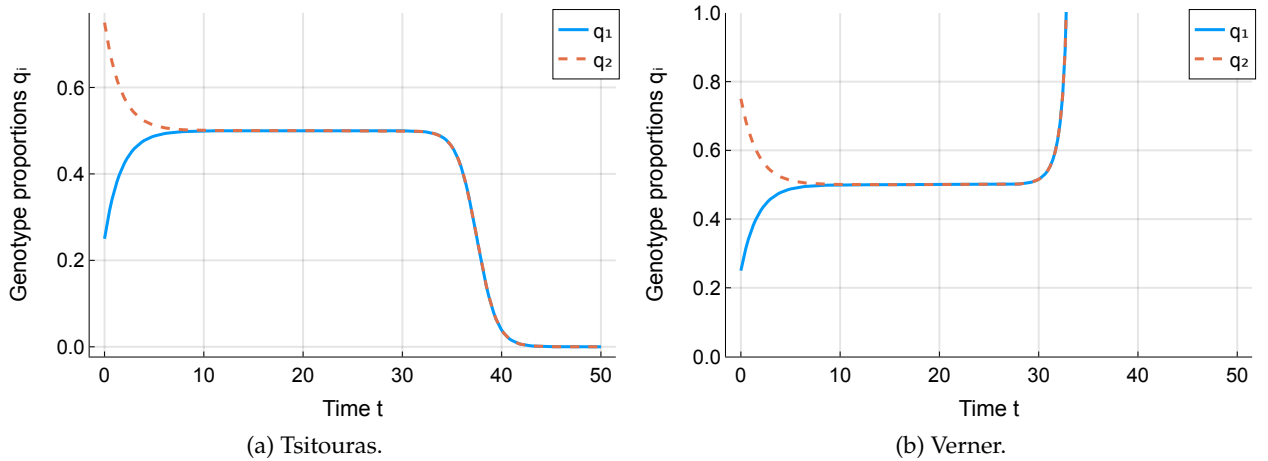


Figure 4: Numerical solution of the system (3.1) with $a = 0.7$ and initial condition $q_0 = (0.25, 0.75)^T$ obtained by the fifth-order Runge-Kutta method of Tsitouras [27] and the sixth-order method of Verner [28] implemented in OrdinaryDiffEq.jl [17] in Julia [2] with absolute and relative tolerances 10^{-8} . For these tolerances, the method of Dormand and Prince [5] yields a numerical solution going to zero.

3.2 Analysis of the 3-component model

Now, we investigate the steady states of the system (2.8), so q^* with $f_i(q^*) = 0$ for $i = 1, 2, 3$.

Solving the equation gives a one-parameter family of non-negative steady states

$$q^* = \left(q_1^*, 2 \left(\sqrt{q_1^*} - q_1^* \right), 1 + q_1^* - 2\sqrt{q_1^*} \right)^T, \quad q_1^* \in [0, 1], \quad (3.2)$$

fulfilling the conservation condition $\sum_{i=1}^3 q_i^* = 1$ and reflecting the binomial distribution of the two alleles. The trivial state $q^* = 0 \in \mathbb{R}^3$ is a steady state as well but does not fulfill the conservation condition.

To investigate the stability properties of the steady states, we compute the eigenvalues of the Jacobian

$$f'(q) = \begin{pmatrix} -1 + 2q_1 + q_2 & q_1 + q_2/2 & 0 \\ q_2 + 2q_3 & -1 + q_1 + q_2 + q_3 & 2q_1 + q_2 \\ 0 & q_2/2 + q_3 & -1 + q_2 + 2q_3 \end{pmatrix}. \quad (3.3)$$

Its eigenvalues are $\lambda_k = -1 + k \sum_{i=1}^3 q_i$, $k \in \{0, 1, 2\}$, with associated eigenvectors

$$v_0 = \begin{pmatrix} 1 \\ -2 \\ 1 \end{pmatrix}, \quad v_1 = \begin{pmatrix} -(2q_1 + q_2) \\ 2(q_1 - q_3) \\ q_2 + 2q_3 \end{pmatrix}, \quad v_2 = \begin{pmatrix} (2q_1 + q_2)^2 \\ 2(2q_1 + q_2)(q_2 + 2q_3) \\ (q_2 + 2q_3)^2 \end{pmatrix}, \quad (3.4)$$

for $q \neq 0$; $f'(0) = -I$ has the eigenvalue -1 with multiplicity three. In particular, the non-trivial steady states are unstable with eigenvalues $-1, 0$, and 1 . The trivial steady state $q^* = 0$ is asymptotically stable. All of these non-negative steady states are visualized in Figure 5.

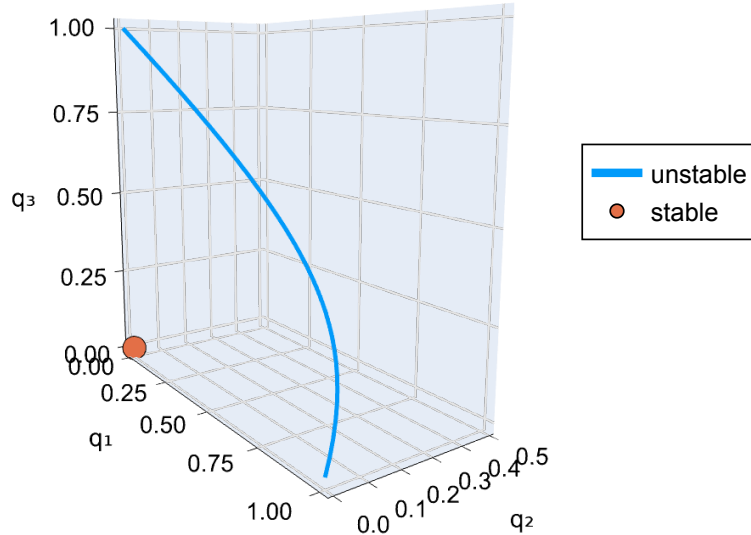


Figure 5: Non-negative steady states of the system (2.8). All non-trivial steady states are unstable.

The dynamical system analysis allows us to answer the first question of why we are having unstable numerical simulations: The steady states on the hyperplane with $\sum_i q_i = 1$ are unstable, both for the 2-component system (3.1) and for the 3-component system (2.8). Useful tools for gaining these information are either the visualization of the dynamical system as a vector field or

the analysis of the eigenvalues of the Jacobian. The preferred method depends on the dimension of the problem.

Small perturbations occurring from floating point errors in the numerical simulations make the system leave the (unstable) hyperplane with $\sum_i q_i = 1$ and the solutions tend to zero or blow up.

The next question is, how we can overcome these difficulties.

4 Using invariants for gaining better models

The systems (2.8) and (3.1) are constructed under the assumption that the total amount $\sum_i q_i = 1$ is conserved. From a modeling perspective, this property seems to remain unchanged for the differential equation system and therefore gives an invariant. Numerical simulations show that $\sum_i q_i$ is not conserved during the simulations. The analysis of the steady states even proves the instability of steady states fulfilling $\sum_i q_i = 1$.

4.1 Qualitative properties of invariants

The question of how to overcome these problems leads us to the analysis of invariants.

Definition 4.1 (First integrals, cf. Section 2.1 of [8]). Let $U \subset \mathbb{R}^M$ be open. Consider the ODE $q' = f(q)$ with $f: U \rightarrow \mathbb{R}^M$. A (time-independent) *first integral* of the ODE is a C^1 -function $J: U \rightarrow \mathbb{R}$ with $J'(q) \cdot f(q) = 0$ for all $q \in U$. The first integral is called *trivial* if $\exists c \forall q \in U: J(q) = c$. \triangleleft

Clearly, a first integral is an invariant of the ODE, i.e., it does not change along a solution trajectory. Indeed, if q solves the ODE $q'(t) = f(q(t))$,

$$\frac{d}{dt}J(q(t)) = J'(q(t)) \cdot q'(t) = J'(q(t)) \cdot f(q(t)) = 0. \quad (4.1)$$

We first prove that the sum $\sum_i q_i$ is not a first integral for (2.8). The functional $J(q) = \sum_i q_i$ has the gradient $(1, 1, 1)^T$. Thus,

$$\begin{aligned} J'(q) \cdot f(q) &= \left(\frac{\partial}{\partial q} \sum_i q_i \right) \cdot f(q) = \sum_i f_i \\ &= q_1^2 + q_2^2 + q_3^2 + 2q_1q_2 + 2q_1q_3 + 2q_2q_3 - q_1 - q_2 - q_3 \\ &= (q_1 + q_2 + q_3)^2 - (q_1 + q_2 + q_3) \neq 0 \end{aligned} \quad (4.2)$$

in general. An analogous result holds for the 2-component model. Thus, the systems (2.8) and (3.1) do not conserve the sum $J(q) = \sum_i q_i$ for all chosen initial values. But once we choose initial values fulfilling $\sum_i q_i = 1$, the analytical solution does not leave the level set of J . Second integrals take this property into account:

Definition 4.2 (Second integrals, cf. Section 2.5 of [8]). Let $U \subset \mathbb{R}^M$ be an open subset. Consider the ODE $q' = f(q)$ with $f: U \rightarrow \mathbb{R}^M$. A *second integral* of the ODE $q'(t) = f(q(t))$ with vector field $f: U \rightarrow \mathbb{R}^M$ is a C^1 -function $J: U \rightarrow \mathbb{R}$ such that there is a function $\alpha: U \rightarrow \mathbb{R}$ satisfying $\forall q \in U: J'(q) \cdot f(q) = \alpha(q)J(q)$. \triangleleft

Clearly, second integrals J are conserved by solutions of the ODE whenever the initial conditions starts on the manifold given by $J(q) = 0$.

The systems (2.8) and (3.1) have the total sum $\sum_i q_i = 1$ as a second integral. The difference $u := \sum_i q_i - 1$ between the total sum and unity satisfies

$$u' = \sum_i q'_i = \left(\sum_i q_i \right)^2 - \left(\sum_i q_i \right) = (1 + u)^2 - (1 + u) = (1 + u)u. \quad (4.3)$$

All Runge-Kutta methods preserve such linear second integrals [26].

The ODE (4.3) is very similar to the ODE of logistic growth and can be solved analytically,

$$u(t) = \frac{u_0}{e^{-t}(1 + u_0) - u_0}, \quad u_0 = u(0). \quad (4.4)$$

This ODE (4.3) has two steady states, the unstable steady state $u = 0$, corresponding to $\sum_i q_i = 1$, and the asymptotically stable steady state $u = -1$ corresponding to $\sum_i q_i = 0$. For an initial condition $u_0 < 0$, $u(t) \rightarrow -1$ for $t \rightarrow \infty$. For initial data $u_0 > 0$, $u(t)$ grows without bounds and blows up in finite time. We discovered this behavior for the 2-component model in Fig. 4.

An initial condition of the original model (2.8) needs to satisfy $\sum_i q_i = 1$. Thus, the system (4.3) is in the unstable steady state. When solving (2.8) numerically, it can be expected that even tiny floating point errors can accumulate over time, either resulting in a blow-up in finite time or a convergence to the biologically meaningless state $\sum_i q_i = 0$. To verify this, we also performed computations using different floating point types. The results shown in Figure 6 are qualitatively the same as before, only the time changes when deviations from the steady state become visible.

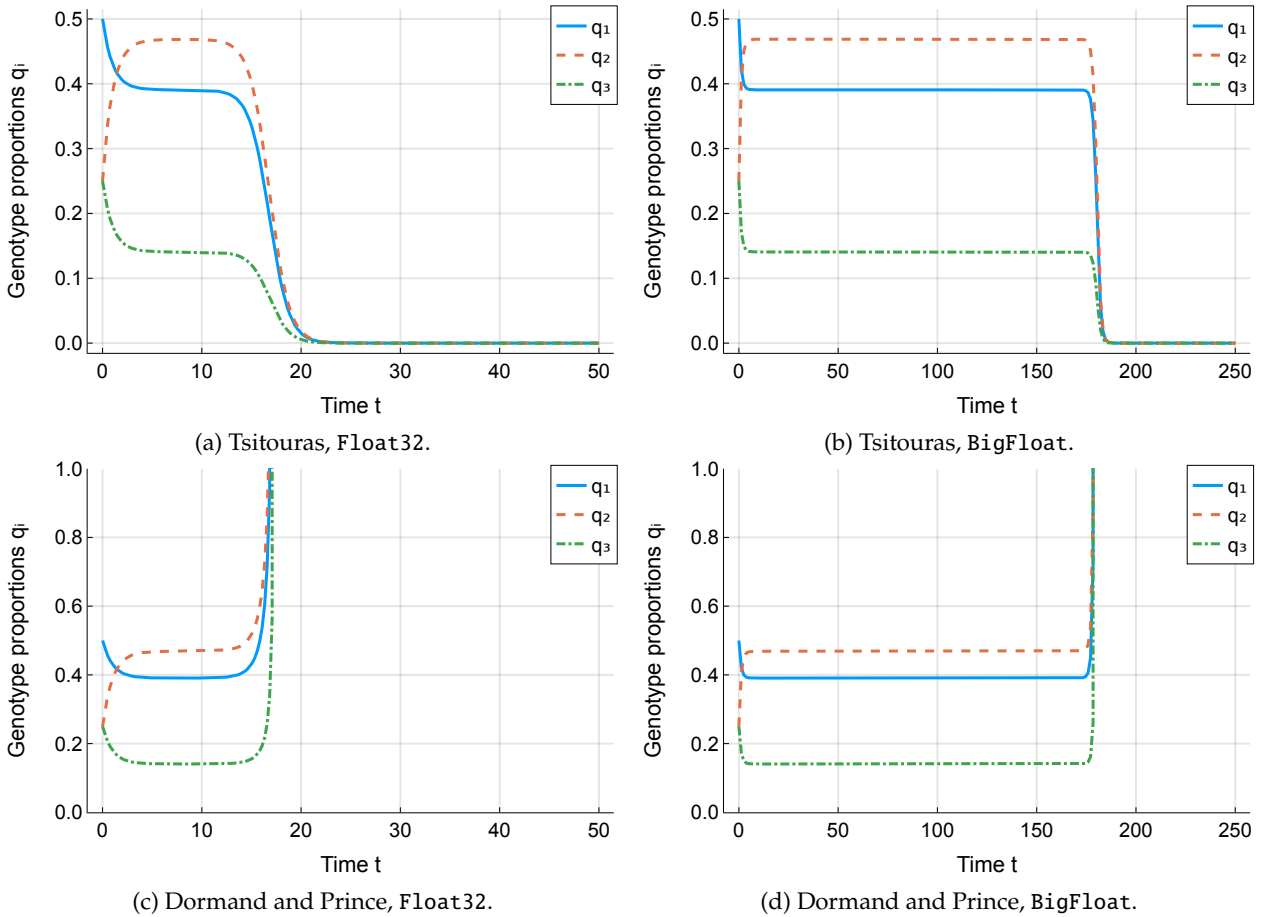


Figure 6: Numerical solution of the system (2.8) with initial condition $q_0 = (0.5, 0.25, 0.25)^T$ obtained by the fifth-order Runge-Kutta methods of Tsitouras [27] and Dormand and Prince [5] implemented in OrdinaryDiffEq.jl [17] in Julia [2] with different floating point types. For 32 bit floating point numbers Float32 we use tolerances 10^{-7} . For high-precision floating point numbers BigFloat, we use stricter tolerances 10^{-14} .

To overcome these issues, we reformulate the system so that the total sum becomes a first integral. First, we present a general result showing that this is possible.

Theorem 4.3. Consider an ODE $q'(t) = f(q(t))$ with affine second integral J . Then, there is a modified

vector field \tilde{f} having J as first integral such that

$$\forall y: J(y) = 0 \implies f(y) = \tilde{f}(y).$$

In particular, the original ODE is equivalent to the modified ODE $\tilde{q}'(t) = \tilde{f}(\tilde{q}(t))$ whenever the initial condition is in the zero set of J . The modified vector field \tilde{f} can be constructed as $\tilde{f}(y) = f(y) - \alpha(y)J'(y)/\|J'(y)\|^2 J(y)$, where we interpret the gradient $J'(y)$ as vector field.

Proof. We have $J'(y) \cdot f(y) = \alpha(y)J(y)$. Choose the ansatz $\tilde{f}(y) = f(y) + J(y)c$ where c is a constant vector that will be suitably chosen. Then,

$$J'(y) \cdot \tilde{f}(y) = J'(y) \cdot f(y) + J(y)J'(y) \cdot c = (\alpha(y) + J'(y) \cdot c) J(y).$$

Since J is affine, $J'(y)$ is constant. If $J'(y) = 0$, $J(y) = c$ and J is already a (trivial) first integral and c can be chosen arbitrarily. Otherwise, choose, e.g., $c = -\alpha(y)J'(y)/\|J'(y)\|^2$ and obtain $J'(y) \cdot \tilde{f}(y) = 0$. Thus, J is a first integral of the vector field \tilde{f} . \square

We will see, that various choices of the coefficient c used in the proof above are possible, leading to different modified models. Further, the modification changes the set of steady states of the ODE leading to different numerical behavior.

4.2 Reformulation of the models

The theory of invariants allows reformulations of the system. The aim is to modify the system in such a way that the stability properties of the steady states improve while retaining the dynamic behavior. We cannot expect to have asymptotically stable steady states but having stable steady states is already an improvement. Then, numerical simulations will be stable and floating point errors do not change the qualitative behavior of the system.

4.2.1 Reformulation of the 2-component model

We start with reformulating the system (3.1) intuitively by using the property $q_1 + q_2 = 1$. First, we reorder the system as

$$q_1' = a q_1^2 + \underbrace{q_1(q_2 - 1)}_{=-q_1} + (1 - a)q_2^2, \quad q_2' = (1 - a)q_1^2 + \underbrace{(q_1 - 1)q_2}_{=-q_2} + a q_2^2. \quad (4.5)$$

Replacing $q_2 - 1 = -q_1$ in the first equation and $q_1 - 1 = -q_2$ in the second gives the new system

$$\begin{aligned} q_1' &= (1 - a)(-q_1^2 + q_2^2), \\ q_2' &= (1 - a)(q_1^2 - q_2^2). \end{aligned} \quad (4.6)$$

In this system, the sum of the components is a first integral since $q_1' + q_2' = 0$ without any further assumptions.

Remark 4.4. The process of changing a dynamical system such that an (affine) second integral becomes a first integral is not unique.

A second integral for system (3.1) is given by $J = u = \sum_i q_i - 1$ in (4.3). Indeed, choosing the function $\alpha(q) = \sum_i q_i$ yields the defining equation $J'(q) \cdot f(q) = \alpha(q)J(q)$. Based on the second integral J we reformulate the system as $\tilde{f}(q) = f(q) + J(q)c$.

Our intuitive approach leading to system (4.6) uses the special choice $c = -q$. We prove by a calculation that the modified system has a first integral: The function $\alpha(q) = \sum_i q_i$ can be written

as $\alpha(q) = J'(q) \cdot q$ with $J(q) = \sum_i q_i - 1$. The new vector field \tilde{f} is given as $\tilde{f}(q) = f(q) - J(q)q$ and the new ODE has a first integral because

$$\frac{d}{dt}J(q(t)) = J'(q) \cdot \tilde{f}(q) = J'(q) \cdot f(q) - J'(q) \cdot J(q)q = \alpha(q)J(q) - J'(q) \cdot J(q)q = 0, \quad (4.7)$$

where we first use the definition of \tilde{f} , then the second integral property of f and thirdly the observation that $\alpha(q) = J'(q) \cdot q$.

On the other hand, the modified vector field \tilde{f} constructed in the proof of Theorem 4.3 with $c = -\alpha(q)J'(q)/\|J'(q)\|^2$ yields the ODE

$$\begin{aligned} q_1' &= \left(aq_1^2 + q_1q_2 + (1-a)q_2^2 - q_1\right) - \frac{1}{2}\left((q_1+q_2)^2 - (q_1+q_2)\right) \\ &= (a-1/2)(q_1^2 - q_2^2) - \frac{1}{2}(q_1 - q_2), \\ q_2' &= \left((1-a)q_1^2 + q_1q_2 + aq_2^2 - q_2\right) - \frac{1}{2}\left((q_1+q_2)^2 - (q_1+q_2)\right) \\ &= (1/2-a)(q_1^2 - q_2^2) + \frac{1}{2}(q_1 - q_2), \end{aligned} \quad (4.8)$$

for the 2-component model (3.1). This is clearly different from (4.6) in general (but of course equivalent on the invariant manifold). \triangleleft

We continue our investigations with the new system (4.6). This system has the non-negative steady states $(q_1^*, q_1^*)^T$ with $q_1^* \geq 0$. For $q_1^* \neq 1/2$, the steady states do not fulfill the condition $\sum_{i=1}^2 q_i = 1$. The vector field is shown in Figure 7. For any initial conditions, the dynamics lead to a steady state $(q_1^*, q_1^*)^T$ with $q_1^* = 1/2(q_1(0) + q_2(0))$.

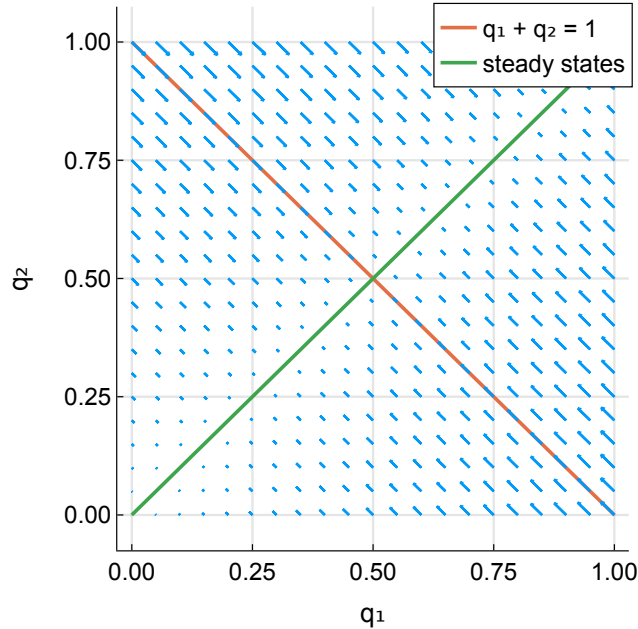


Figure 7: Visualization of the right-hand side vector field f of the modified 2-component system (4.6) with $a = 0.7$. The invariant manifold given by $q_1 + q_2 = 1$ is highlighted. The length of the lines is proportional to $\sqrt{\|f(q)\|}$.

The stability of the steady states can be assured by calculating the eigenvalues of the Jacobian of the system. The Jacobian

$$f'(q) = 2(1-a) \begin{pmatrix} -q_1 & q_2 \\ q_1 & -q_2 \end{pmatrix} \quad (4.9)$$

has the eigenvalues $\lambda_0 = 0$ and $\lambda_1 = -2(1-a)(q_1 + q_2) < 0$ with eigenvectors

$$v_0 = \begin{pmatrix} q_2 \\ q_1 \end{pmatrix}, \quad v_1 = \begin{pmatrix} -1 \\ 1 \end{pmatrix}, \quad (4.10)$$

for $q \neq 0$; $f'(0) = 0$ has the double eigenvalue 0. Consequently, the non-trivial steady states are stable.

Starting with any initial values $q_1, q_2 > 0$, the solutions tend towards the steady states. If the initial conditions fulfill the condition $\sum_i q_i = 1$ of the hyperplane, the solutions remain on the hyperplane. Deviations on the manifold, for example caused by floating point errors, will not change the overall system behavior and result in deviations of the steady state from the hyperplane. For this model, a transformation of variables to $p_1 = q_1 + q_2$ and $p_2 = q_2 - q_1$ separates the tendency towards the hyperplane from the stationary behavior on the manifold but would change the interpretability of the variables.

Remark 4.5. The stability of steady states of the modified 2-component system (4.6) can be understood easily by looking at Figure 7.

This behavior is also generic in the sense that it can be obtained from the center manifold theorem — at least locally, see [10, Theorem I.4] or [14, Theorem 2.7]. Summarized briefly, the center manifold theorem states that a dynamical system near a steady state where all eigenvalues of the Jacobian have a non-negative real part behaves as follows: i) There is a neighborhood V of the steady state and a manifold M of the same dimension as the generalized eigenspace associated with eigenvalues on the imaginary axis that is invariant under the flow as long as the evolving state stays in V . ii) If the state stays in V for all times, it converges (exponentially) to the manifold M . In our case, the eigenvalue on the imaginary axis is zero and the corresponding manifold is the set of steady states. \triangleleft

In this particular example, a stable model can be derived as well by including the manifold equation $1 = q_1 + q_2$ directly into (4.6). Then, the system becomes decoupled and $q'_1 = (1-a)(1-2q_1)$ is a single equation describing the evolution without any interpretable mechanisms. This reduction step does not follow the intention of highlighting the interplay between modeling, analysis and numerical simulation, so we will not discuss it further.

4.2.2 Reformulation of the 3-component model

Inserting the conservation condition $\sum_{i=1}^3 q_i = 1$ into the first equation of (2.8) yields

$$q'_1 = q_1^2 + q_1 q_2 + \frac{1}{4} q_2^2 - q_1 \underbrace{(q_1 + q_2 + q_3)}_{=1} = \frac{1}{4} q_2^2 - q_1 q_3. \quad (4.11)$$

Continuing this process for the other equations as well results in the modified system

$$\begin{aligned} q'_1 &= \frac{1}{4} q_2^2 - q_1 q_3, \\ q'_2 &= -\frac{1}{2} q_2^2 + 2q_1 q_3, \\ q'_3 &= \frac{1}{4} q_2^2 - q_1 q_3. \end{aligned} \quad (4.12)$$

Again, as in the case of the 2-component model, this reformulation can be interpreted as turning the second integral $J(q) = u(q) = \sum_i q_i - 1$ with $\alpha(q) = \sum_i q_i$ into a first integral for the new vector field $\tilde{f} = f - J(q)q$. The calculations in Remark 4.4 are valid as well for the 3-component system.

The modified system (4.12) has the non-negative steady state $q^* = (q_1^*, q_2^*, q_3^*)^T$ with

$$q_3^* = \begin{cases} \text{arbitrary} \geq 0, & \text{if } q_1^* = q_2^* = 0, \\ \frac{q_2^{*2}}{4q_1^*}, & \text{if } q_1^* \neq 0, \end{cases} \quad (4.13)$$

for $q_1^*, q_2^* \geq 0$ and $q_2^* = 0$ if $q_1^* = 0$. Note in particular that the steady states of (4.12) satisfying $\sum_i q_i = 1$ are exactly the non-trivial steady states of the original system (2.8). The Jacobian is

$$f'(q) = \begin{pmatrix} -q_3 & q_2/2 & -q_1 \\ 2q_3 & -q_2 & 2q_1 \\ -q_3 & q_2/2 & -q_1 \end{pmatrix}. \quad (4.14)$$

For $q \neq 0$, $f'(q)$ has a double eigenvalue $\lambda_0 = \lambda_1 = 0$ with eigenspace spanned by

$$v_0 = \begin{pmatrix} q_1 \\ 0 \\ -q_3 \end{pmatrix}, \quad v_1 = \begin{pmatrix} q_2/2 \\ q_1 + q_3 \\ q_2/2 \end{pmatrix}, \quad (4.15)$$

as well as the eigenpair

$$\lambda_2 = -\sum_{i=1}^3 q_i, \quad v_2 = \begin{pmatrix} 1 \\ -2 \\ 1 \end{pmatrix}. \quad (4.16)$$

Moreover, $f'(0) = 0$. Thus, all non-negative steady states are associated with eigenvalues of $f'(q)$ with non-positive real parts. The non-negative steady states are visualized in Figure 8.

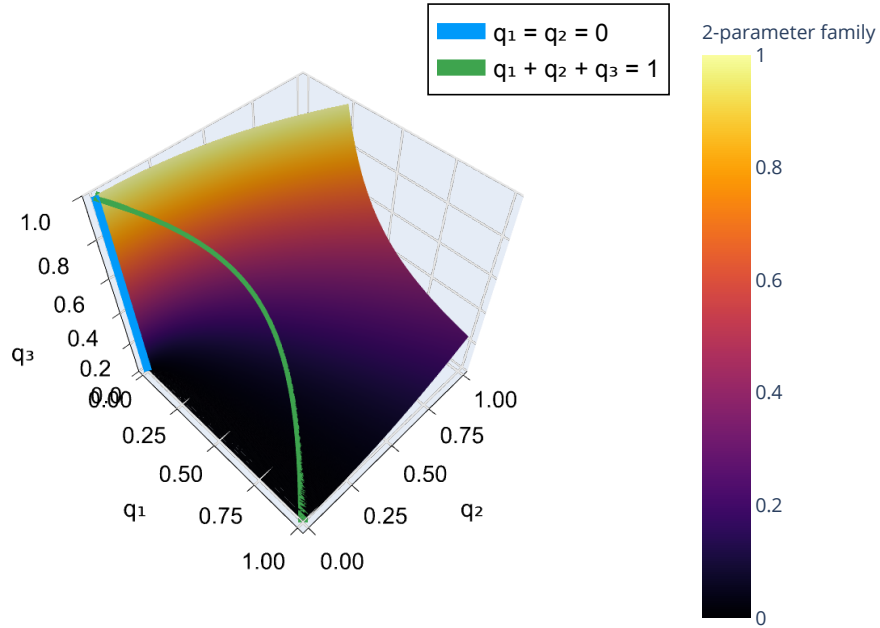


Figure 8: Non-negative steady states of the system (4.12). The system Jacobian has only eigenvalues with non-positive real parts at all steady states.

As expected based on this stability analysis, numerical solutions behave properly when applied to the modified systems (4.6) and (4.12). This is demonstrated in Figure 9.

The modified systems (4.6) and (4.12) have stable steady states fulfilling $\sum_i q_i^* = 1$. The modification of the reaction functions changes the system's properties from having a second integral to having a first integral.

5 Evaluation of the models

After improving the analytical properties and ensuring the conservation of $\sum_i q_i$ during the numerical simulations, we like to draw attention to the modeling process.

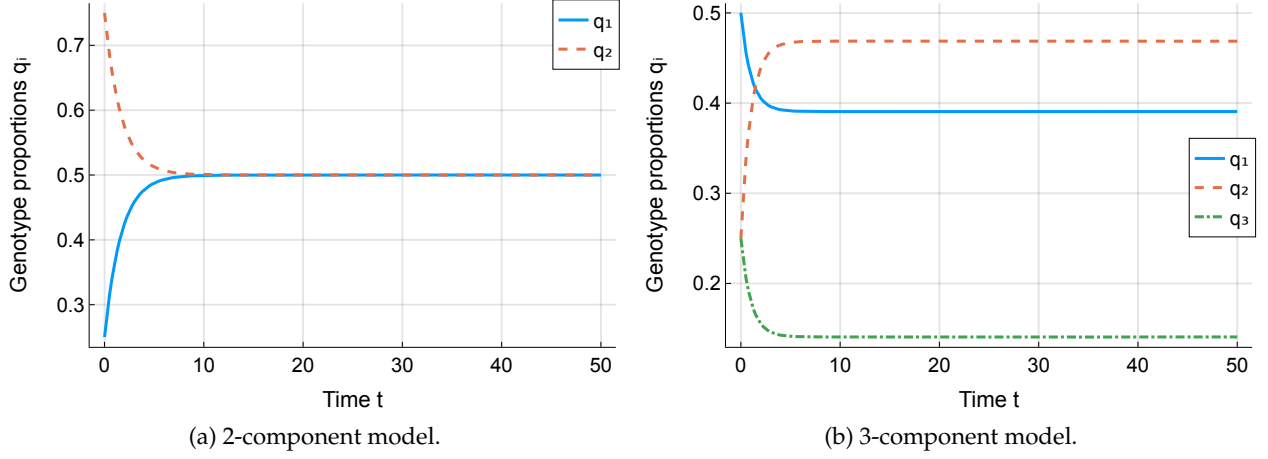


Figure 9: Numerical solution of the modified systems (4.6) (with $a = 0.7$ and initial condition $q_0 = (0.25, 0.75)^T$) and (4.12) (with initial condition $q_0 = (0.75, 0.25, 0.25)^T$) obtained by the fifth-order Runge-Kutta method of Tsitouras [27] implemented in OrdinaryDiffEq.jl [17] in Julia [2] with absolute and relative tolerances 10^{-8} .

The models (2.8) and (3.1) were derived quite directly from the biological application. The system quantities q_k give the proportion of genotype k in the total population. The condition $\sum_i q_i = 1$ arises therefore naturally from the biological application and the mathematical translation into equations. The biologically motivated models surprised us during the numerical simulations with their unstable behavior arising from leaving the hyperplane with $\sum_i q_i = 1$. Floating point errors already lead to unstable behavior, resulting in solutions tending towards zero or blowing up.

We used the conservation property to reformulate the ordinary differential equation systems. The new systems (4.6) and (4.12) have the same dynamics on the hyperplane as the original models (2.8) and (3.1).

Summarized, the new models were derived based on analytical considerations and not according to a modeling process. In general, changing the functions of a model might result in differential equations without any (obvious and direct) connection to the modeling object. Here, we try to interpret the inheritance of genes in the new model (4.12).

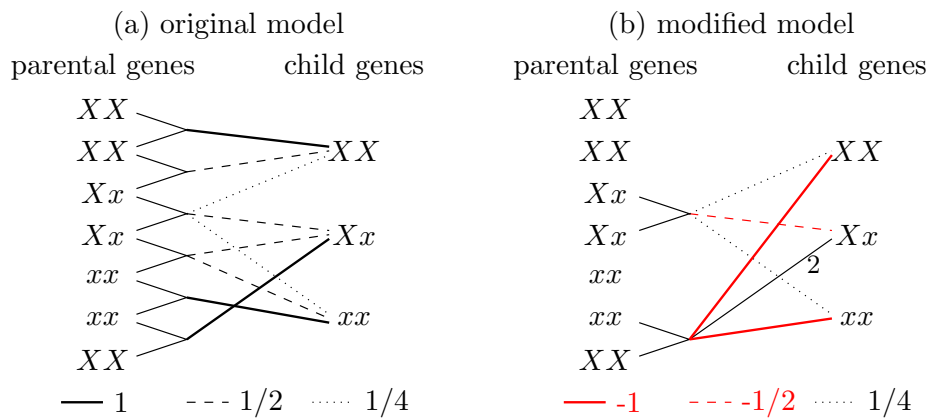


Figure 10: Modeled combinations of genes in the original system (2.8) and the modified system (4.12).

While the system (2.8) translates all combinations of parental genes into equations, the modified system (4.12) regards fewer combinations. The modified system includes only the combination of the mixed genotype Xx and the combination of the two pure genotypes. The combination of two pure genotypes of the same type is not modeled. This can be interpreted as neglecting combinations that do not change the proportions of genotypes in the population. This affects as well the combination q_2 of two genotypes, since the factor $-1/2$ is the difference between the actual

factor $1/2$ in system (2.8) and the factor 1 symbolizing the preservation of genotype q_2 .

The change from system (2.8) to the modified system (4.12) is a change in the point of view: While the first model describes the random assortment of genotypes from the point of view of the parental generation, the new model focuses on the change of proportions. In our case, only those combinations are included in the model that change the proportions of the genotypes in the population. Leveling effects, like the inheritance of genotype q_1 with probability $1/2$ if q_1 and q_2 are combined and therefore $1/2$ of the parental genes are identical to the child genes, are not modeled.

A similar interpretation is possible for the 2-component model. As the modified system (4.6) only regards the change of the proportions, the pure conservation of one proportion is not regarded.

Interpretations like this are not automatically possible if a model with a second integral is turned into a model with a first integral. In any case, the new formulation might reveal new perspectives on the application and the most relevant mechanisms in the mathematical description.

6 Conclusion — or what can we learn?

The example we discussed in this article shows how surprising numerical simulation results may lead to insightful analysis and reformulation of mathematical models. The reformulation gives insight into properties of the modeled application on two levels. First, the reformulation process itself sheds light on conservation properties of the model. Second, the new formulation may change the view on the model leading to new interpretations of the mechanisms. Gaining insight into underlying principles is complicated for large models. The proposed reformulation workflow may support the finding of hidden principles while improving the analytical and numerical properties.

Please note that we neither blame the numerics nor the modeling; it is their combination that lead to the catastrophic behavior we discussed. If it was affordable to use exact representations of all numbers occurring in the numerical time integration process, we could just use the original model. However, this is only possible for small problems and short time scales, e.g., by using rational numbers with high-precision integer types such as `Rational{BigInt}` in Julia. However, it appears to be preferable for us to adapt the modeling process, thereby avoiding the unrealistic instabilities inherent in the original model. This is required for most practical purposes, e.g., if uncertainties are present or larger-scale simulations are used.

To recap, a surprising behavior of numerical methods applied to an innocently looking model from mathematical biology for studying genetic drift guided us on a tour through several undergraduate and graduate courses including mathematical modeling, dynamical systems, and numerical analysis. In particular, we had a chance to see the importance of invariants and their manifestation in first and second integrals as well as stability properties of steady states.

We would like to see this article as a bridge gathering results and techniques from several basic courses together while motivating advanced courses in applied mathematics. This includes for example deeper concepts of stability analysis, the study of asymptotic behavior of dynamical systems [15, 22], and advanced results such as the center manifold theorem [10, 14] or Fenichel's theory on invariant manifolds [7] on the theoretical side. The latter emphasizes using transformation to local coordinates on the manifold. While this approach has many analytical benefits, local coordinates are oftentimes difficult to interpret in the context of applications.

From the point of view of a numerical analyst, it stresses the importance of structure-preserving numerical methods, introduced in textbooks such as [9, 21] in the context of numerical methods for ODEs; the corresponding partial differential equation topics appear to be more specialized and available mostly in form of journal articles such as [6, 18, 19, 25]. The basic reason for us to modify the mathematical models was to stabilize the dynamics when the total sum is not equal to unity. This is related to invariant-preserving numerical methods such as the orthogonal projection approach described in [9, Section IV.4]. However, most numerical analysts would probably not consider using such tools here since we only need to preserve a linear functional — which the standard time integration methods we employ do automatically [26] — at least in exact arithmetic.

Thus, the behavior is somewhat surprising but of course well understood after performing a stability analysis. In some sense, we have to deal with non-ideal versions in practice while the common analysis assumes ideal numerical methods. This happens also in many other cases in practice, e.g., if iterative numerical methods are used to solve equations arising in implicit time integration schemes [3, 12, 13].

We introduced the problem of invariants and manifolds in the context of mathematical biology. Of course, problems of this type occur in many applications, for example in control problems [29] or mechanical systems [9]. Finally, we encourage researchers in the field of mathematical modeling and applied sciences to discover the strength of mathematical theory, especially for dynamical systems and for structure-preserving numerical schemes, for gaining insight into the dynamics of interest.

To make this study reproducible and useful for classroom teaching, we provide all source code and instructions available online in our repository [20] — in the form of an interactive notebook using the modern programming language Julia.

Acknowledgments

We would like to thank Dirk Langemann for discussions about this topic and constructive comments on an early draft of the manuscript.

HR was supported by the Deutsche Forschungsgemeinschaft (DFG, German Research Foundation, project number 513301895) and the Daimler und Benz Stiftung (Daimler and Benz foundation, project number 32-10/22).

References

- [1] B. Allen and A. McAvoy. “A mathematical formalism for natural selection with arbitrary spatial and genetic structure.” In: *J. Math. Biol.* 78.4 (2019), pp. 1147–1210. doi: 10.1007/s00285-018-1305-z.
- [2] J. Bezanson, A. Edelman, S. Karpinski, and V. B. Shah. “Julia: A Fresh Approach to Numerical Computing.” In: *SIAM Rev.* 59.1 (2017), pp. 65–98. doi: 10.1137/141000671.
- [3] P. Birken and V. Linders. “Conservation Properties of Iterative Methods for Implicit Discretizations of Conservation Laws.” In: *J. Sci. Comput.* 92.2 (2022), pp. 1–32.
- [4] N. F. Britton. *Essential mathematical biology*. Springer Undergraduate Mathematics Series. London: Springer, 2003. doi: 10.1007/978-1-4471-0049-2.
- [5] J. R. Dormand and P. J. Prince. “A family of embedded Runge-Kutta formulae.” In: *J. Comput. Appl. Math.* 6.1 (1980), pp. 19–26. doi: 10.1016/0771-050X(80)90013-3.
- [6] H. Egger. “Structure preserving approximation of dissipative evolution problems.” In: *Numer. Math.* 143.1 (2019), pp. 85–106. doi: 10.1007/s00211-019-01050-w.
- [7] N. Fenichel and J. K. Moser. “Persistence and Smoothness of Invariant Manifolds for Flows.” In: *Indiana Univ. Math. J.* 21.3 (1971), pp. 193–226. URL: <http://www.jstor.org/stable/24890380>.
- [8] A. Goriely. *Integrability and nonintegrability of dynamical systems*. Vol. 19. Advanced series in nonlinear dynamics. World Scientific, 2001.
- [9] E. Hairer, C. Lubich, and G. Wanner. *Geometric Numerical Integration: Structure-Preserving Algorithms for Ordinary Differential Equations*. Vol. 31. Springer Series in Computational Mathematics. Berlin Heidelberg: Springer-Verlag, 2006. doi: 10.1007/3-540-30666-8.
- [10] G. Iooss and M. Adelmeyer. *Topics in Bifurcation Theory and Applications*. Vol. 3. Advanced series in nonlinear dynamics. Singapore: World Scientific, 1998.

- [11] D. Langemann, O. Richter, and A. Vollrath. “Multi-gene-loci inheritance in resistance modeling.” In: *Math. Biosci.* 242.2013 (2012), pp. 17–24. doi: 10.1016/j.mbs.2012.11.010.
- [12] V. Linders and P. Birken. “Locally conservative and flux consistent iterative methods.” In: *SIAM Journal on Scientific Computing* (2024), S424–S444. doi: 10.1137/22M1503348.
- [13] V. Linders, H. Ranocha, and P. Birken. “Resolving Entropy Growth from Iterative Methods.” In: *BIT Numerical Mathematics* 63 (4 Sept. 2023). doi: 10.1007/s10543-023-00992-w. arXiv: 2302.13579 [math.NA].
- [14] J. E. Marsden and M. McCracken. *The Hopf Bifurcation and Its Applications*. Vol. 19. Applied Mathematical Sciences. New York: Springer, 1976.
- [15] L. Perko. *Differential equations and dynamical systems*. 3rd ed. Texts in applied mathematics 7. New York: Springer, 2001.
- [16] F. van der Plas, M. Dral, P. Berg, et al. *fonsp/Pluto.jl: v0.19.20*. Version v0.19.20. Jan. 2023. doi: 10.5281/zenodo.5889169. URL: <https://doi.org/10.5281/zenodo.5889169>.
- [17] C. Rackauckas and Q. Nie. “DifferentialEquations.jl – A Performant and Feature-Rich Ecosystem for Solving Differential Equations in Julia.” In: *J. Open Res. Softw.* 5.1 (2017), p. 15. doi: 10.5334/jors.151.
- [18] H. Ranocha, D. Mitsotakis, and D. I. Ketcheson. “A Broad Class of Conservative Numerical Methods for Dispersive Wave Equations.” In: *Commun. Comput. Phys.* 29.4 (Feb. 2021), pp. 979–1029. doi: 10.4208/cicp.0A-2020-0119. arXiv: 2006.14802 [math.NA].
- [19] H. Ranocha, M. Sayyari, L. Dalcin, M. Parsani, and D. I. Ketcheson. “Relaxation Runge-Kutta Methods: Fully-Discrete Explicit Entropy-Stable Schemes for the Compressible Euler and Navier-Stokes Equations.” In: *SIAM J. Sci. Comput.* 42.2 (Mar. 2020), A612–A638. doi: 10.1137/19M1263480. arXiv: 1905.09129 [math.NA].
- [20] C. Reisch and H. Ranocha. *Reproducibility repository for Modeling still matters: a surprising instance of catastrophic floating point errors in mathematical biology and numerical methods for ODEs*. https://github.com/ranocha/2023_modeling_matters. Apr. 2023. doi: 10.5281/zenodo.7801250.
- [21] J. M. Sanz-Serna and M. P. Calvo. *Numerical Hamiltonian Problems*. Vol. 7. Applied Mathematics and Mathematical Computation. London: Chapman & Hall, 1994.
- [22] R. Seydel. *Practical Bifurcation and Stability Analysis*. Vol. 5. Interdisciplinary Applied Mathematics. New York, NY: Springer New York, 2010. doi: 10.1007/978-1-4419-1740-9.
- [23] L. F. Shampine and M. W. Reichelt. “The MATLAB ODE suite.” In: *SIAM J. Sci. Comput.* 18.1 (1997), pp. 1–22. doi: 10.1137/S1064827594276424.
- [24] J. D. Skufca. “Analysis Still Matters: A Surprising Instance of Failure of Runge-Kutta-Felberg ODE Solvers.” In: *SIAM Rev.* 46.4 (2004), pp. 729–737. doi: 10.1137/S003614450342911X.
- [25] E. Tadmor. “Entropy stability theory for difference approximations of nonlinear conservation laws and related time-dependent problems.” In: *Acta Numer.* 12 (2003), pp. 451–512. doi: 10.1017/S0962492902000156.
- [26] B. K. Tapley. *On the preservation of second integrals by Runge-Kutta methods*. 2021. arXiv: 2105.10929 [math.NA].
- [27] C. Tsitouras. “Runge-Kutta pairs of order 5 (4) satisfying only the first column simplifying assumption.” In: *Comput. Math. Appl.* 62.2 (2011), pp. 770–775. doi: 10.1016/j.camwa.2011.06.002.
- [28] J. H. Verner. “Numerically optimal Runge-Kutta pairs with interpolants.” In: *Numer. Algorithms* 53.2-3 (2010), pp. 383–396. doi: 10.1007/s11075-009-9290-3.

- [29] R. A. Wehage and E. J. Haug. "Generalized Coordinate Partitioning for Dimension Reduction in Analysis of Constrained Dynamic Systems." In: *J. Mech. Des.* 104.1 (1982), pp. 247–255. doi: 10.1115/1.3256318.